Double Vortex Flows in Plasmas Axially Traversing Multipole Magnetic Fields

GERALD O. BARNEY* AND J. C. SPROTT
Department of Physics, University of Wisconsin
Madison, Wisconsin
(Received 25 June 1968; final manuscript received 10 October 1968)

Detailed observations of 100-eV hydrogen plasmas moving in a linear quadrupole and a toroidal octupole magnetic field show that the plasmas polarize and that the field lines quickly become equipotentials. The plasmas $\mathbf{E} \times \mathbf{B}$ drift with negligible diamagnetism in double vortex flow patterns similar to the self-consistent solutions of Poukey. The agreement is not perfect presumably because the uniform field and steady state assumed in the theory are lacking in the experiments.

INTRODUCTION

The behavior of a plasma moving transverse to a magnetic field has been studied theoretically by Poukey[1,2] in the following idealized situation: (1) steady state; (2) straight uniform magnetic field, infinite in extent; (3) collisionless plasma; (4) drift velocity small compared with the thermal velocity[3]; and (5) small gyroradii.[3] When these conditions are met, Poukey has shown that the magnetic field, density, pressure, and perpendicular energy are constant on lines of equipotential in the frame of reference moving with the plasma, and that the plasma can exhibit a characteristic double vortex or convection cell flow pattern. One vortex has a positive potential and the other a negative potential.

Vortex flow patterns have previously been observed and reported by several authors.[4-7] The present paper describes detailed observations of vortices observed in the Wisconsin toroidal octupole[8] and linear quadrupole.[9] Although Poukey's assumptions are not well satisfied, the experimental results resemble the predictions of his theory.

In both experiments, potentials are measured with high-impedance floating probes. Because of the fast time variation of potentials ($\sim$1 μsec), special care must be taken to insure that the probe follows the potential fluctuations, especially at low densities. The method used is to place a high resistance near the probe tip to attenuate the signal and reduce the effective probe capacitance.[10] Density measurements were made with a special type of floating double probe described in Ref. 10.

Rather than look at the potential at every point in space, it is more convenient to measure the potential as a function of time in a plane perpendicular to the bulk velocity $\mathbf{v}_0$ of the plasma. The velocity $\mathbf{v}_0$ is determined from the time of flight between two such planes, and the time coordinate can then be converted to a distance along the direction of motion of the plasma.

In comparing the experimental and theoretical results, it is convenient to transform the observed potential contours into a frame of reference moving with velocity $\mathbf{v}_0$ in which the contours are also flow lines. The transformation equation is given by

$$-\nabla V_l - \frac{1}{c}\frac{\partial \mathbf{A}_l}{\partial t} = -\nabla V_m - \frac{1}{c}\frac{\partial \mathbf{A}_m}{\partial t} + \frac{1}{c}\mathbf{v}_0 \times \mathbf{B}, \quad (1)$$

where V and $\mathbf{A}$ are the plasma and magnetic vector potentials and the subscripts l and m refer to the laboratory and moving frames, respectively. Experimentally, the plasmas show negligible diamagnetism, so $\mathbf{A}_l$ and $\mathbf{A}_m$ are assumed to be time independent. Also, assuming the plasma temperature to be independent of position and time, ∇V_l can be replaced by the gradient of the floating potential ∇V_f. In the two-dimensional case, Eq. (1) can then be simplified and integrated to give the potential at position s and time t:

$$V_m(s, t) = V_f(s, t) + \frac{1}{c}\int_0^s \mathbf{v}_0 \times \mathbf{B}(\mathbf{s}) \cdot d\mathbf{s}. \quad (2)$$

Equation (2) is used to transform the observed potential contours into the moving frame.

* Present address: Analyses Group, Center for Naval Analyses, Arlington, Virginia.
[1] J. W. Poukey, Bull. Am. Phys. Soc. 11, 452 (1966).
[2] J. W. Poukey, Phys. Fluids 10, 2253 (1967).
[3] This assumption can be relaxed considerably.
[4] W. H. Bostick, Phys. Fluids 6, 1958 (1963).
[5] W. H. Bostick, in *Proceedings of the Seventh International Conference on Phenomena in Ionized Gases* (Gradevinska Knjiga, Beograd, Yugoslavia, 1966), Vol. 2, p. 141.
[6] D. R. Wells, Phys. Fluids 9, 1010 (1966).
[7] W. H. Bostick, Phys. Fluids 9, 2078 (1966).
[8] A. Filimonov, D. E. Lencioni, J. C. Sprott, and R. L. Willig, Jr., Bull. Am. Phys. Soc. 11, 452 (1966).
[9] G. O. Barney, Bull. Am. Phys. Soc. 11, 452 (1966).
[10] J. C. Sprott, Rev. Sci. Instr. 37, 897 (1966).

TABLE I. Comparison of quadrupole and octupole experiments.

	Quadrupole	Octupole
Plasma source	Coaxial gun	Conical gun
Type of plasma	Hydrogen	Hydrogen
Streaming velocity (V_0)	$\sim 1.4 \times 10^7$ cm/sec	$\sim 6.5 \times 10^6$ cm/sec
Electron temperature	~ 10 eV	10 eV
Plasma density	$> 7.5 \times 10^{12}$ cm^{-3}	$\sim 10^{10}$ cm^{-3}
Ion–ion collision time	100 μsec	100 msec
Peak field strength in midplane	600 G	1.9 kG

The main characteristics of the two experiments are listed in Table I.

LINEAR QUADRUPOLE EXPERIMENT

After moving through a 1-m long field-free drift space, the plasma stream enters the quadrupole field and moves along the field axis parallel to the rods. The floating potential measurements are made during the transit of the stream. A flux plot of the quadrupole field is shown in Fig. 1. The entering plasma stream sharply cuts off 12-mm microwave transmission indicating a peak density in excess of 7.5×10^{12} cm^{-3}. The plasma expands around the rods making the field lines equipotentials. Magnetic probe measurements show negligible diamagnetism: $\Delta B/B \approx 1\%$. The proton gyroradius is comparable to the distance over which the field changes appreciably.

Floating potential measurements with high impedance probes are made along straight lines AA and BB indicated in Fig. 1. The stationary probes look at different parts of the plasma cloud as it moves by. The time coordinate is converted to a distance along the direction of cloud travel by multiplying the time by the streaming velocity $\mathbf{v}_0$. The velocity $\mathbf{v}_0$ in the quadrupole case is determined to be 1.4×10^7 cm/sec by measuring the time required for the potential contours to propagate between two positions in the direction of cloud travel.

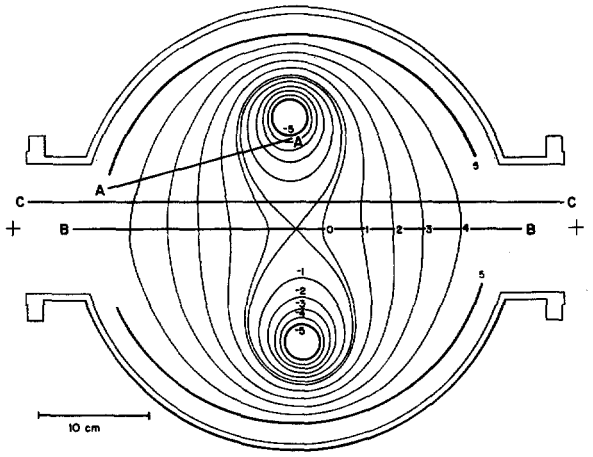

FIG. 1. Wisconsin linear quadrupole flux plot. There are 780 G cm per flux tube per centimeter length along the axis. Straight lines A, B, and C indicate where floating potential scans were made.

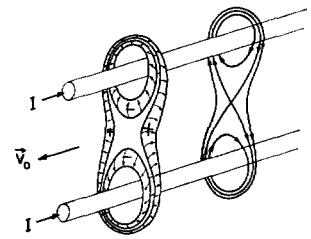

FIG. 2. Schematic illustration of complete double vortex flow pattern observed in the Wisconsin linear quadrupole.

An extension of Poukey's configuration to a three-dimensional quadrupole field is illustrated in Fig. 2. Note that the inner vortices encircle separate rods whereas the outer vortex encircles both rods.

Potential contours observed in the rod-to-wall scan (see Fig. 1) are shown in Figs. 3(a) and (b) for the laboratory frame and the moving frame, respectively. Although the negative vortex is much smaller than the positive one, the double-vortex structure is clearly seen in the laboratory frame. This asymmetry probably results from a combination of factors not considered by Poukey such as transient effects,

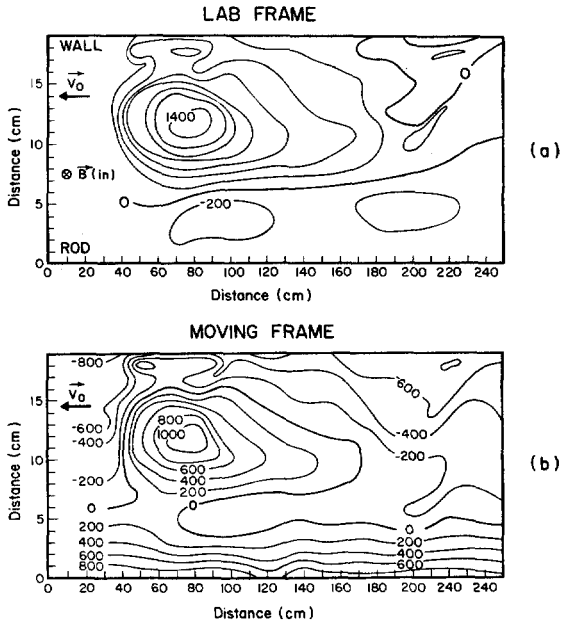

FIG. 3. Equipotentials observed in the quadrupole rod-to-wall scan in the lab frame (a) and moving frame (b). Potentials are in volts.

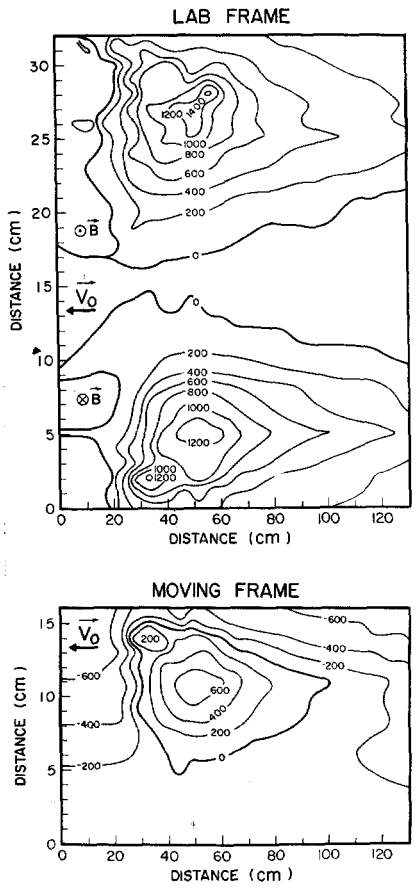

FIG. 4. Equipotentials observed in the quadrupole midplane scan in the lab frame (a) and moving frame (b). Potentials are in volts.

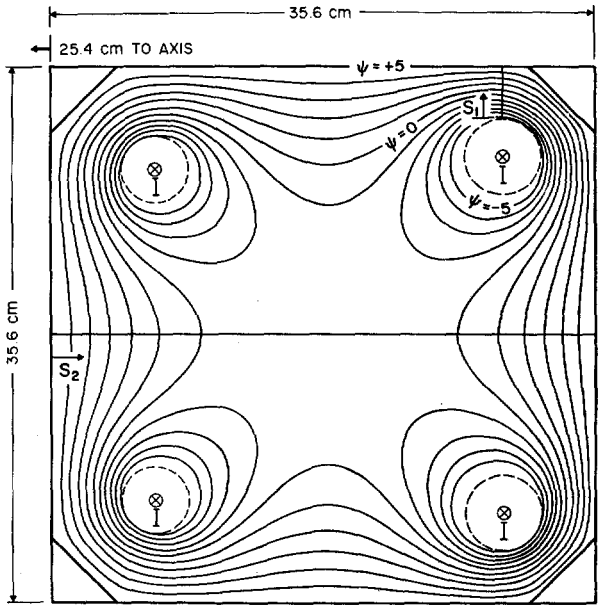

FIG. 5. Computer calculated magnetic flux plot of a cross section of the Wisconsin toroidal octupole field in a constant θ plane. S_1 and S_2 indicate the lines along which probe scans were made.

grounding of the plasma by charge flow along the separatrix to the wall, curvature of the field, and the very large particle orbits near the field axis. The vortex near the rod is actually present in the moving frame, but it does not appear in Fig. 3(b) because of the choice of the contour interval. The structure beyond the 140-cm mark is influenced by the collision with the end of the system. The third small vortex at the stream front near the wall may be due to the abrupt distortion in the field at the wall discontinuity. Both the inner and outer vortices encircle the rod. Both sides of the outer vortex can be seen in the midplane scan shown in Fig. 4. The symmetry is quite good. Localized density measurements were not possible in the quadrupole because of instrumental difficulties with the probes in the presence of the high-density plasma.

When plasma is injected perpendicular to the field axis, a double vortex forms in the region just inside the injection port, expands along the field lines over the rods and finally separates into two streams moving parallel and antiparallel to the rod currents.[11] The positive potentials in the stream moving antiparallel to the rod currents are much larger than the negative potentials in the oppositely directed stream. Current flow along field lines prevents $\mathbf{E} \times \mathbf{B}$ drift of the stream out through the field region directly opposite the injection port. Time resolved potential contours[12] from data collected after many highly reproducible shots show that the plasma strikes the end of the system and then moves back toward the injection port. The interaction of the incoming and reflected streams produces a relatively large diamagnetic effect. This process is merely a result of the finite length of the system and must not be confused with diamagnetic injection.

TOROIDAL OCTUPOLE EXPERIMENT

In the toroidal octupole,[13] the azimuthal coordinate θ is defined such that plasma enters the field at $\theta = 0°$, splits into two clouds traveling in the $+\theta$ and $-\theta$ directions, and collides at $\theta = 180°$. A computer-calculated magnetic flux plot of a cross section of the octupole field in a constant θ plane is shown in Fig. 5. The magnetic field lines are numbered from $\psi = -5$ at the rods to $\psi = +5$ at the

[11] G. O. Barney, Bull. Am. Phys. Soc. **12**, 494 (1967).
[12] G. O. Barney, Ph.D. thesis, University of Wisconsin (1967).
[13] R. A. Dory, D. W. Kerst, D. M. Meade, W. E. Wilson, and C. W. Erickson, Phys. Fluids **9**, 997 (1966).

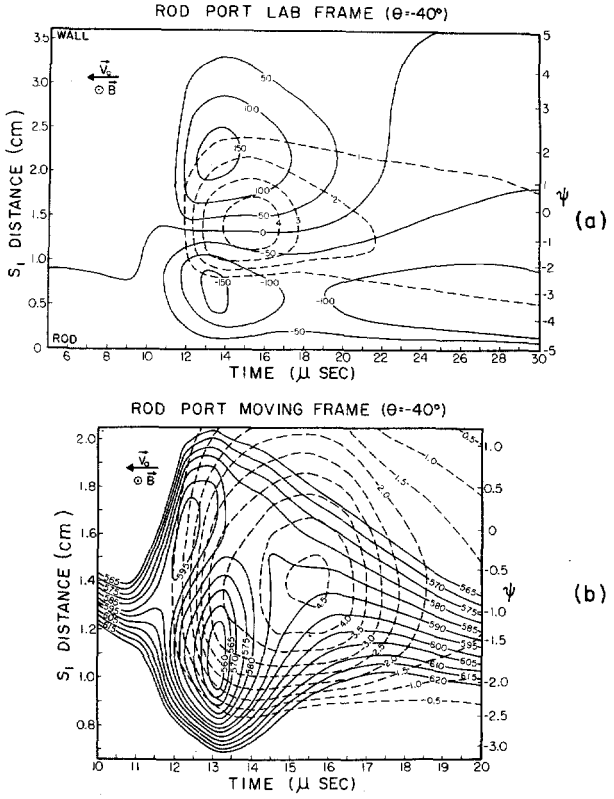

FIG. 6. Equipotential (solid) and equal density (dashed) contours observed in the octupole rod-to-wall scan in the lab frame (a) and moving frame (b). Potentials are in volts and densities in units of $\sim 10^{10}$ cm^{-3}. One microsecond corresponds to a circumferential distance of about 8 cm.

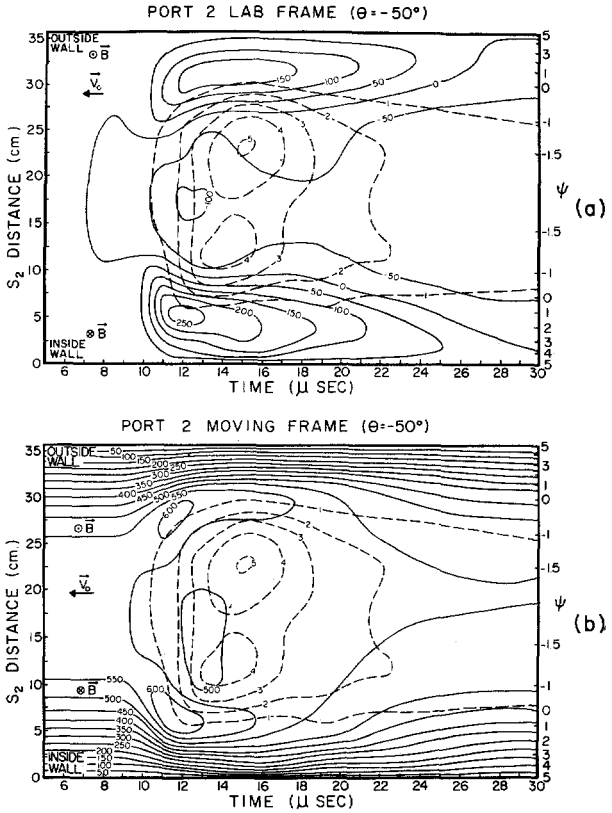

FIG. 7. Equipotential (solid) and equal density (dashed) contours observed in the octupole midplane scan in the lab frame (a) and moving frame (b) at 50° around the circumference of the toroid from the injection port. Near the center, 1 μsec corresponds to a circumferential distance of about 6.5 cm.

walls. The magnetic field **B** is given by

$$\mathbf{B} = \frac{\alpha}{R}\,\hat{\theta} \times \nabla\psi,$$

where R is the distance to the major axis of the toroid and α is a constant having a value of 6.1×10^4 G cm^2 for ψ defined as in Fig. 5.

For density and potential constant on a magnetic field line, measurements as a function of ψ and time uniquely determine the motion of the plasma. The observed potentials and densities along the line labeled S_1 in Fig. 5 are shown in Fig. 6(a). Note that the $\mathbf{E} \times \mathbf{B}$ drift is in the direction of $\mathbf{v}_0$ at the center and opposite to $\mathbf{v}_0$ near the walls and rods. In the laboratory system, the plasma exhibits the double vortex flow pattern described by Poukey. The density, however, shows only one peak, in contrast to the two predicted. Measurements of the cloud traveling in the opposite direction from the injection port show similar contours except that the sign of the potentials is reversed.

In order to convert the laboratory potentials into the moving frame, it is necessary to measure the angular velocity $\omega = v_0/R$ of the plasma in the θ direction. This was accomplished by three different methods: (1) The time required for the plasma to propagate between two ports was determined by measuring the density and potential in the horizontal midplane (S_2 in Fig. 5) at $\theta = -50°$ and at $\theta = -113°$. Figures 7(a) and 8(a) show the result. There is a slight distortion of the potentials and a considerable elongation of the density contours as the plasma moves between the two ports, indicating that a steady state has not been reached. Note that the potential contours appear to propagate with a velocity about three times faster than the velocity of the density peaks, in contradiction to Poukey's theory. (2) The instanteous bulk velocity of the plasma was determined by evaluating $\omega = cE_s/RB$ at the density peak in Fig. 6(a). (3) The center-of-mass angular velocity was determined from the contours in Fig. 6(a) by assuming that the density and potential are constant on a magnetic field line and using

$$\omega = c \int \frac{E_s R}{B} n\, d^3r \Big/ \int R^2 n\, d^3r$$
$$= c \int \left(\int \frac{\partial V_f}{\partial s} \frac{n(\psi, t)}{RB}\, dt \right) \cdot \left(\oint \frac{R^2\, dl}{B} \right) d\psi \Big/ \int \left(\int n(\psi, t)\, dt \right) \left(\oint \frac{R^2\, dl}{B} \right) d\psi, \quad (3)$$

where l is an element of length parallel to **B**. The time integration in Eq. (3) was taken from 12 to 20 μsec. All three methods give a value of $\omega = 1.5 \times 10^5$ sec^{-1}. The laboratory potential contours were then converted to the moving frame by substituting $v_0 = \omega R$ and $B = (\alpha/R)\,|\nabla\psi|$ into Eq. (2) giving

$$V_m(\psi, t) = V_f(\psi, t) + \frac{1}{c} \int_0^s \omega\alpha\, |\nabla\psi|\, ds$$
$$= V_f(\psi, t) - (1/c)\alpha\omega(\psi - \psi_0). \quad (4)$$

Using Eq. (4) with $\psi_0 = +5$, the laboratory frame potentials in Figs. 6(a), 7(a), and 8(a), were transformed into the moving frame. Figures 6(b), 7(b), and 8(b) show the result. Note that the density contours are not affected by the transformation. The transformation moves the circulation centers toward one another and makes the circulation less pronounced.

Note that it is always possible to transform into a frame of reference moving so fast that the vortices do not appear. Had a larger transformation velocity been used, such as the propagation velocity of the potential contours, as was done in the quadrupole case, closed contours would not have been obtained in the moving frame, and plasma would move backwards at every point in space.

It is also possible to choose a frame such as is given by the spatial average of E_s/RB

$$\omega = c \int \frac{E_s}{RB}\, d^3r \Big/ \int d^3r$$
$$= c \int \left(\int \frac{\partial V_f}{\partial s} \frac{1}{RB}\, dt \right) \cdot \left(\oint \frac{dl}{B} \right) d\psi \Big/ \int \left(\int dt \right) \left(\oint \frac{dl}{B} \right) d\psi.$$

This method gives a smaller value of $\omega \cong 5.6 \times 10^3$ sec^{-1}. Using this value to convert the laboratory frame potentials into the moving frame gives potential contours almost identical to those of Fig. 6(a). This ambiguity in choosing a unique velocity results in part from the fact that the plasma is not in a steady state and that potential and density are not constant on a magnetic field line. In the uniform field case considered by Poukey, all of the above methods for calculating the moving frame velocity would give identical results.

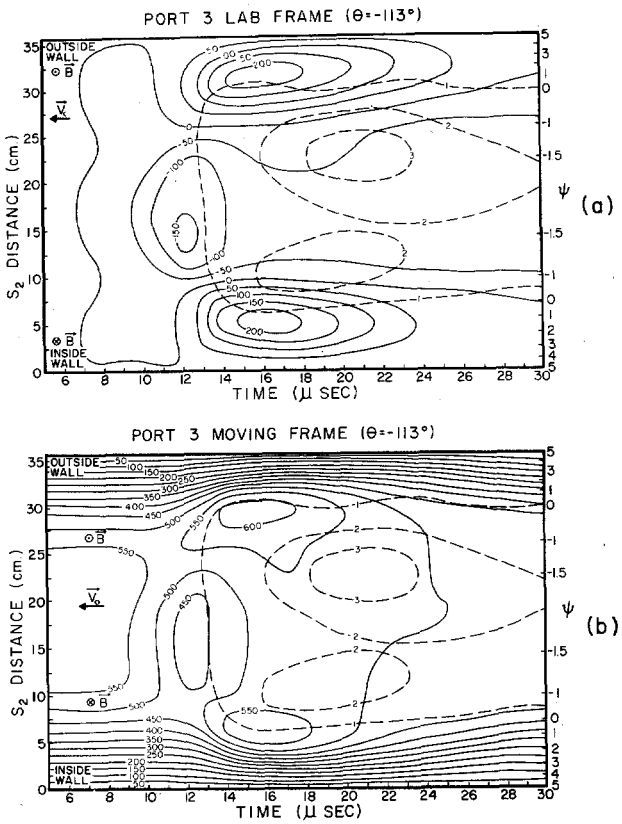

FIG. 8. Equipotential (solid) and equal density (dashed) contours observed in the octupole midplane scan in the lab frame (a) and moving frame (b) at 113° around the circumference of the toroid from the injection port. Near the center, 1 μsec corresponds to a circumferential distance of about 6.5 cm.

For a uniform magnetic field, Poukey has shown that a steady-state solution exists in which the density is constant on an equipotential in the moving frame. In the case of a nonuniform field such as a closed line multipole, a more general condition may be derived. In the zero temperature limit where the velocity is given by $c\mathbf{E} \times \mathbf{B}/B^2$, the continuity equation requires that, in the moving frame, in which equipotentials are flow lines, the flux of particles between equipotential V_m and $V_m + \delta V$ must be constant along the equipotential. The flux at each point is given by

$$nw\, \delta A = \oint \frac{ncE_m}{B} \frac{\delta V}{\nabla V_m}\, dl = nc\, \delta V \oint \frac{dl}{B}.$$

Since δV is constant along the equipotential, we obtain the result that $n \oint dl/B$ is constant on an equipotential in the moving frame. Note that for

a uniform field $\oint dl/B = \text{const}$, and the above result reduces to that obtained by Poukey. For a pure toroidal field, the condition reduces to $n/B^2 = \text{const}$, a result previously obtained by Daugherty and Levy[14]. For a multipole, $\oint dl/B$ is infinite on the separatrix and hence a steady state can exist only if the density goes to zero there.

In Figs. 6(b), 7(b), and 8(b), it is apparent that the quantity $n \oint dl/B$ is not even approximately constant on an equipotential. The density has a single peak near the separatrix ($\psi = -1.6$) and tends to lag behind the potential peaks. As shown previously, such a configuration cannot represent a steady state in which the velocity is given by $c\mathbf{E} \times \mathbf{B}/B^2$. If the ion ∇B drift is taken into account, the result would be to increase the electric field at the forward boundary of the plasma and cause the plasma to $\mathbf{E} \times \mathbf{B}$ drift toward the low-field region in analogy with the outward drift in a pure toroidal magnetic field. In a toroidal magnetic field, a neutral plasma moves radially outward with an initial acceleration given by[15]

$$a = \frac{2k(T_i + T_e)}{M_i R}.$$

This result can be generalized to an arbitrary closed magnetic field geometry.[16] The result is

$$a = \frac{k(T_i + T_e)\,\partial/\partial\psi \oint dl/B}{M_i B \oint dl/B^3}. \tag{5}$$

For the toroidal octupole, Eq. (5) predicts that the plasma moves in toward the separtrix in a time short compared with the time required for the plasma to $\mathbf{E} \times \mathbf{B}$ drift around the vortex.

The consistency of the potential and density data can in principle be tested by applying the continuity equation

$$\nabla \cdot n\mathbf{v} = c\,\frac{\mathbf{E}\times\mathbf{B}}{B^2}\cdot\left(\nabla n - 2n\,\frac{\nabla B}{B}\right) = -\frac{\partial n}{\partial t} \tag{6}$$

at every point in space. If the potentials and density propagate with the same velocity (v_0) and are constant on a field line, Eq. (6) reduces to

$$\frac{\partial V_f}{\partial t}\left(\frac{\partial n}{\partial s} - \frac{2n}{B}\frac{\partial B}{\partial s}\right) + \frac{\partial n}{\partial t}\left(\frac{Bv_0}{c} - \frac{\partial V_f}{\partial s}\right) = 0. \tag{7}$$

Equation (7) is satisfied everywhere only if the potential and density peaks coincide in the moving frame as is the case for Poukey's solutions. When Eq. (7) is applied to the experimental contours, continuity is satisfied near the density peak, but not on the edges of the density profile. This result is consistent with the experimental observations that at the front of the plasma cloud there is a net flow of plasma from the minor axis into the narrow region between the rods and the wall and that a steady state has not been reached.

Extensive tests on the behavior of plasma transported around the toroid in the presence of an added toroidal magnetic field of $B_\theta \cong 360$ G were made and reported elsewhere.[17,18]

CONCLUSIONS

In both the quadrupole and octupole, double vortex flow patterns are seen during the transport of the plasma. The agreement with Poukey's solutions is not perfect, however, presumably because the field is very nonuniform and because a steady state does not exist. It may be that we are observing the first stages in the evolution of vortices, and that given sufficient time a steady state would develop more closely resembling that described by Poukey.

It is interesting to note that these vortices can exist with any bulk velocity including one that is zero in the laboratory frame, and that their rotational velocity is arbitrary. The persistent localized fluctuations observed in some multipoles[19–21] may be examples of such stationary vortices. These vortices ought to be more pronounced in quadrupoles than in octupoles because the ∇B drifts which push plasma toward the separatrix are smaller in quadrupoles. In any case, vortices would tend to circulate plasma from the separatrix out to regions near the rods and wall where it could subsequently be lost.

ACKNOWLEDGMENTS

The authors gratefully acknowledge the guidance of Dr. D. W. Kerst under whose direction this work was done. Dr. D. M. Meade and Dr. J. W. Poukey contributed valuable discussion. D. E. Lencioni developed the probes which were used for the density measurements, and D. Marshall performed much of the computer work.

This work was supported by the United States Atomic Energy Commission.

[14] J. D. Daugherty and R. H. Levy, Phys. Fluids **10**, 155 (1967).
[15] P. C. T. van der Laan, J. Nucl. Energy **C6**, 559 (1964).
[16] D. M. Meade, Phys. Fluids **11**, 2497 (1968).
[17] J. C. Sprott, Bull. Am. Phys. Soc. **12**, 789 (1967).
[18] D. E. Lencioni, J. W. Poukey, J. A. Schmidt, J. C. Sprott, and C. W. Erickson, Phys. Fluids **11**, 1115 (1968).
[19] M. Roberts, I. Alexeff, and W. Halchin, Phys. Letters **26A**, 590 (1968).
[20] T. Ohkawa and M. Yoshikawa, Phys. Rev. Letters **19**, 1374 (1967).
[21] R. W. Palladino and S. Yoshikawa, Phys. Fluids **11**, 1820 (1968).